Inorg. Chem. **2003**, *42*, 4724–4730

Structure of AuCN Determined from Total Neutron Diffraction

Simon J. Hibble,*,† Alex C. Hannon,‡ and Simon M. Cheyne†,‡

School of Chemistry, University of Reading, Reading RG6 6AD, U.K., and ISIS Facility, Rutherford Appleton Laboratory, Chilton, Didcot, OX11 0QX, U.K.

Received February 24, 2003

The structure of gold cyanide, AuCN, has been determined at 10 and 300 K using total neutron diffraction. The structure consists of infinite –Au–(CN)–Au–(CN)–Au–(CN)– linear chains, hexagonally packed, with the gold atoms in sheets. The Au–C and Au–N bond lengths are found to be identical, with $d_{Au-C/N} = 1.9703(5)$ Å at 300 K. This work supersedes a previous study, by others, which used Rietveld analysis of neutron Bragg diffraction in isolation, and found these bonds to have significantly different lengths ($\Delta d = 0.24$ Å) at 300 K. The total correlation function, *T(r)*, at 10 and 300 K, has been modeled using information derived from total diffraction. The broadening of inter- and intrachain correlations differs markedly due to random displacements of the chains in the direction of the chain axes. This is a consequence of the relatively weak bonding between the chains. An explanation for the negative thermal expansion in the *c*-direction, which occurs between 10 and 300 K, is presented.

Introduction

For such apparently simple systems, definitive structures of the metal cyanides, MCN, where M is Cu, Ag, or Au, have proved remarkably elusive. As recently as 1998, Bowmaker et al.[1] used neutron Bragg diffraction to determine for the first time the light atom positions in AgCN and confirmed that the structure consists of infinite −Ag−(CN)−Ag−(CN)− chains arranged on a hexagonal grid, as found by West.[2] In the same work Bowmaker et al.[1] determined a detailed structure for AuCN.[1] The structures of AuCN and AgCN differ in the way the chains are packed together. In the case of AuCN the metal atoms are in layers, whereas in AgCN the metal atoms in neighboring chains are displaced along the chain axis by one-third of the chain repeat distance. The structure of AuCN, as determined by Bowmaker et al.,[1] is shown in Figure 1. It has been suggested that the reason AuCN adopts this arrangement of chains is that this minimizes the Au−Au distance and leads to a favorable aurophilic interaction.[1]

We recently redetermined the structure of the disordered crystalline material, AgCN, using total neutron diffraction.[3]

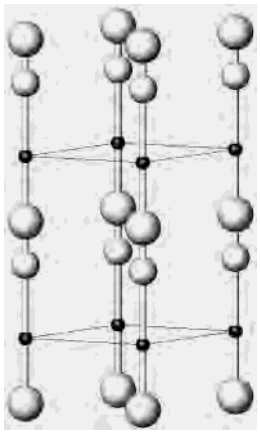

Figure 1. Structure of AuCN (small atoms Au, large atoms C, medium atoms N) after Bowmaker et al.[1] Light lines indicate the unit cell, and the *c* axis lies up the page.

The total correlation function, $T(r)$, obtained by Fourier transforming the total neutron diffraction pattern, showed that the Ag−C and Ag−N bond lengths were identical, $d_{Ag-C/N} = 2.06$ Å at 10 K, in contrast to the values of $d_{Ag-C} = 2.15$ Å and $d_{Ag-N} = 1.86$ Å found by Bowmaker et al. at room temperature. Combining our result with an analysis of the Bragg diffraction, we were able to produce a model which explained both the average and local structure in AgCN, as described below. Using similar methods, we have determined

* Authors to whom correspondence should be addressed. S.J.H. Fax: 44 118 3786331; Tel: 44 118 3786315; E-mail: s.j.hibble@rdg.ac.uk. A.C.H. Fax: 44 1235 445720; Tel: 44 1235 445358; E-mail: a.c.hannon@rl.ac.uk.

† University of Reading.

‡ Rutherford Appleton Laboratory.

(1) Bowmaker, G. A.; Kennedy, B. J.; Reid, J. C. *Inorg. Chem.* **1998**, *37*, 3968.

(2) West, C. D. *Z. Krystallogr.* **1934**, *88*, 173. West, C. D. *Z. Krystallogr.* **1935**, *90*, 173.

(3) Hibble, S. J.; Cheyne, S. M.; Hannon, A. C.; Eversfield, S. G. *Inorg. Chem.* **2002**, *41*, 1042.

10.1021/ic0342043 CCC: $25.00
Published on Web 06/25/2003

that one polymorph of CuCN, α-CuCN, adopts the same structure as AgCN, albeit in an even more highly disordered form.[4] This confirmed that α-CuCN contains linear $(-Cu(C-N)-)_\infty$ chains, as has been suggested previously on the basis of earlier EXAFS,[5] and NMR and NQR studies.[6] A notable feature of α-CuCN is that, as in AgCN, the M−C and M−N bond lengths are identical, $d_{Cu-C/N} = 1.846$ Å at 10 K. This is not what one would expect from a naive picture of chemical bonding.

In both AgCN and α-CuCN there are no chemical bonds between the chains. The weak interactions between chains means that they can easily slip against each other. This slippage, which is greatest in CuCN, produces a large degree of interchain disorder in the two materials. This disorder affects both the intensities and widths of Bragg reflections and is not easily modeled in Rietveld analysis. It is this disorder that leads to the failure of conventional Rietveld analysis in determining the structure of AgCN and CuCN. An additional source of disorder in these materials is head to tail disorder of the CN groups, as has been found using NMR.[6,7] Unfortunately, because the M−C and M−N bond lengths are identical, our total neutron diffraction studies have a very low sensitivity to head to tail disorder of the CN groups in these metal cyanides.

The very high thermal parameters reported for Au and N, and the large difference in the temperature factors for C and N determined by Bowmaker et al.,[1] led us to the conclusion that AuCN must also be disordered. We therefore suspected that the structure of AuCN determined by conventional Rietveld analysis of the Bragg diffraction was not correct, and that reinvestigation using total neutron diffraction[8] might prove profitable. We were particularly interested to discover whether the Au−C and Au−N bond lengths, $d_{Au-C} = 2.06$ Å and $d_{Au-N} = 1.82$ Å, determined by Bowmaker et al.[1] were correct. Total neutron diffraction experiments were carried out using the GEM[9] diffractometer at the ISIS Facility at the Rutherford Appleton Laboratory, which has a very large range in momentum transfer, Q ($=2\pi/d$). These yield total correlation functions with good resolution in real-space. This allows a direct measurement of interatomic distances to be made, without any of the assumptions inherent in the normal crystallographic analysis of Bragg diffraction, in which a single unit cell is used to describe both the average and local structure. The high reciprocal-space resolution of GEM[9] also allows us to carry out conventional Rietveld analysis, and thus determine the average structure of a crystalline material. For disordered crystalline materials, the goal is to produce a model that can account for both the local structure seen in the total correlation function, and the average structure determined from Bragg diffraction.[8] Below, we report the local and average structures of AuCN at 10 and 300 K, determined using the total diffraction data collected on GEM.

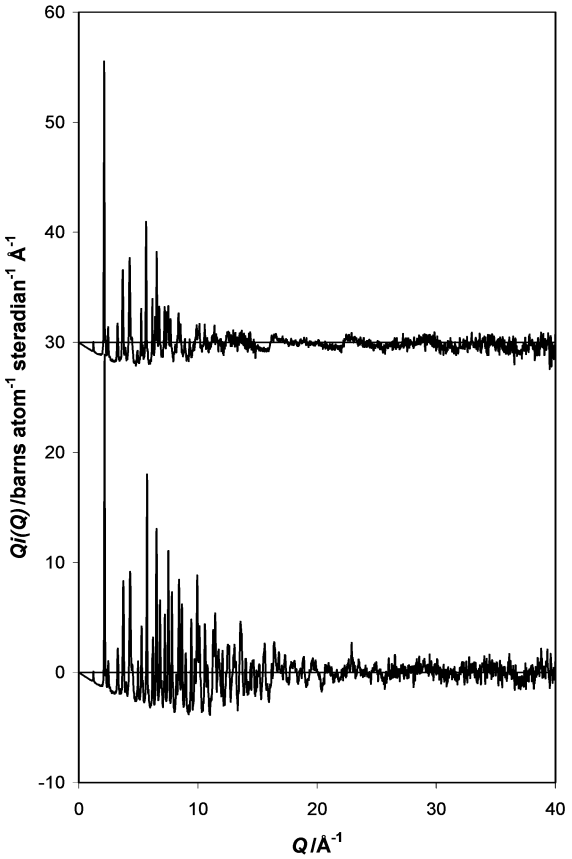

Figure 2. Interference function, $Qi(Q)$, for AuCN at 10 K (bottom) and 300 K (top, displaced vertically by 30 units).

Results and Discussion

Total Diffraction. The interference function, $Qi(Q)$, for AuCN at 10 and 300 K is shown in Figure 2. The Bragg diffraction peaks are clearly visible out to $Q \sim 20$ Å^{-1} in the 10 K data set, and to $Q \sim 12$ Å^{-1} in the 300 K data set. The more rapid decay with Q of the Bragg reflections in the higher temperature data set is a consequence of greater disorder, including larger thermal motions at 300 K. Another notable feature in the 300 K data set is the saw-tooth diffuse scattering, visible above 15 Å^{-1}, which resembles that seen for AgCN[3] and CuCN,[4] and is a characteristic feature for one-dimensional chains. The low r region of the total correlation function, $T(r)$, obtained via a Fourier transformation of the interference function,[8] is shown in Figure 3.

Peaks in $T(r)$ correspond to frequently occurring interatomic distances in the sample. The peak around 1.15 Å can be ascribed to the C−N distance, and that around 1.97 Å can be ascribed to both Au−C and Au−N correlations. The structure determined by Bowmaker et al.[1] gives significantly different Au−C and Au−N bond distances of $d_{Au-C} = 2.06$ Å and $d_{Au-N} = 1.82$ Å, and hence is in error. The internuclear distances obtained by fitting the peaks in $T(r)$ at around 1.15

(4) Hibble, S. J.; Cheyne, S. M.; Hannon, A. C.; Eversfield, S. G. *Inorg. Chem.* **2002**, *41*, 4990.
(5) Stemmler, T. L.; Barnhart, T. M.; Penner-Hahn, J. E.; Tucker, C. E.; Knochel, P.; Böhme, M.; Frenking, G. *J. Am. Chem. Soc*. **1995**, *117*, 12489.
(6) Kroeker, S.; Wasylishen, R. E.; Hanna, J. V. *J. Am. Chem. Soc*. **1999**, *121*, 1582.
(7) Bryce, D. L.; Wasylishen, R. E. *Inorg. Chem.* **2002**, *41*, 4131.
(8) Hibble, S. J.; Hannon, A. C.; Fawcett, I. D. *J. Phys.: Condens. Matter* **1999**, *11*, 9203.
(9) Hannon, A. C. In *Encyclopedia of Spectroscopy and Spectrometry*; Lindon, J., Tranter, G., Holmes, J., Eds.; Academic Press: London, 2000; vol. 2, p 1479.

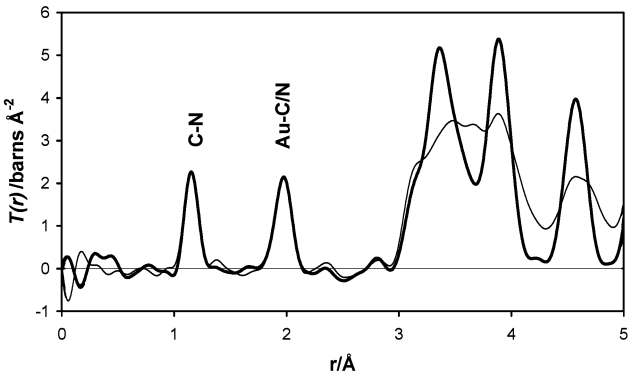

Figure 3. Experimental correlation function, $T(r)$ for AuCN at 10 K (thick line) and 300 K (thin line).

Table 1. Parameters Obtained from Fitting the First Two Peaks in the Total Correlation Function, $T(r)$, for AuCN at 10 and 300 K, the Derived Chain Repeat Distance, and Parameters Derived from Rietveld Profile Refinement

	10 K	300 K
r_{C-N}/Å from $T(r)$	1.1547(4)	1.1499(2)
d_{C-N}/Å from Rietveld	1.144(2)	1.140(2)
$\langle u_{C-N}^2\rangle^{1/2}$/Å from $T(r)$	0.022(1)	0.028(1)
$\langle u_{C-N}^2\rangle^{1/2}$/Å from Rietveld	0.129(2)	0.212(1)
$r_{Au-C/N}$/Å from $T(r)$	1.9717(5)	1.9703(5)
$d_{Au-C/N}$/Å from Rietveld	1.969(1)	1.966(1)
$\langle u_{Au-C/N}^2\rangle^{1/2}$/Å from T($r$)	0.051(1)	0.052(1)
$\langle u_{Au-C/N}^2\rangle^{1/2}$/Å from Rietveld	0.121(2)	0.224(2)
chain repeat distance ($r_{C-N} + 2r_{Cu-C/N}$)/Å derived from $T(r)$	5.098(1)	5.090(1)
c parameter/Å from Rietveld	5.08238(5)	5.07256(3)
a parameter/Å ($= d_{Au-Au}$) from Rietveld	3.3426(1)	3.3915(1)

and 1.97 Å are given in Table 1. The C−N bond length, r_{C-N} = 1.155 Å, which we obtain by fitting $T(r)$, is significantly shorter than the value, d_{C-N} = 1.21 Å, determined from Rietveld refinement by Bowmaker et al.[1] and is in good agreement with the values we found in AgCN[3] and CuCN.[4]

The peaks in $T(r)$ arising from both C−N and Au−C/N correlations are narrow. The peak at around 1.15 Å due to the C−N correlation is especially narrow ($\langle u_{C-N}^2\rangle^{1/2} \sim 0.02-0.03$ Å), and this reflects the strong triple bond between C and N in the cyanide group. The narrow width of the correlation due to Au−C/N shows that any difference in the Au−C and Au−N bond lengths must be extremely small. There is no evidence for any splitting of the 1.97 Å peak at 10 or 300 K. The first two peaks in $T(r)$ change very little in position or width on heating from 10 to 300 K. However, the appearance of $T(r)$ beyond 3 Å changes dramatically when the temperature is raised, and the peaks become much broader. To account for $T(r)$ in this region, a model has to be constructed, considering that beyond the first two peaks more than one pair of atoms normally contribute to the overall correlation function, $T(r)$, and a simple assignment of peaks to individual pairs of atoms is in general impossible. To do this, we use information obtained from Rietveld analysis of the Bragg scattering, see below.

We emphasize that the correlation function, $T(r)$, gives information on interatomic distances directly and is not model dependent. In conventional analysis of Bragg diffraction, an average unit cell is used to describe the periodic structure, and the assumption is normally made that this also gives an accurate description of the local structure. This is not always the case, as we[8] and others[10] have shown in the past. Indeed, conventional analysis of Bragg diffraction for CuCN and AgCN fails in this respect, as discussed above. In the case of CuCN and AgCN, we were able to account for the failure of conventional Bragg diffraction to produce an accurate local structure in terms of the disorder in the materials. This disorder was evident in the appearance of the interference function, $Qi(Q)$. In contrast, the interference function for AuCN at 10 K does not immediately suggest a high degree of disorder, although the 300 K data are reminiscent of the CuCN and AgCN data, showing saw-tooth diffuse scattering. We therefore considered it useful to carry out conventional Rietveld analysis of the Bragg diffraction data to determine whether it would produce the correct local structure for AuCN, and, if not, to gain an insight into why it failed to yield the correct answer.

Rietveld Refinements. Three different models were used to describe the average structure and refined using the Rietveld method. The refined atomic displacement factors are given as root-mean-square displacements, $\langle u^2\rangle^{1/2}$, to enable easy comparison with the values used to broaden interatomic correlations in the $T(r)$ models. The root-mean-square displacement, $\langle u^2\rangle^{1/2}$, is related to the commonly used B values for Bragg diffraction via

$$B = 8\pi^2 \langle u^2\rangle \quad (1)$$

Model A. In our initial refinement we used as a starting model the structure of AuCN determined by Bowmaker et al. in space group $P6mm$.[1] In model A, carbon and nitrogen are on different sites and the CN groups are ordered head to tail along the metal−cyanide chains, as shown in Figure 1. This model was very unstable when used to fit the 10 K data set and converged only when we constrained the carbon and nitrogen thermal displacement factors to be equal. We obtained the structural parameters given in Table 2.

Model B. In this model, we initially placed carbon and nitrogen on positions 0,0,z and 0,0,−z and constrained the shift on z_C to be equal to minus the shift on z_N. This ensured that the Au−C and Au−N bond lengths were equal, as found from total diffraction, and remained so during the refinement. This model retains $P6mm$ symmetry and head to tail ordering of the CN groups.

Model C. In this model, we gave each of the two nonmetal sites 50/50 occupancy of carbon and nitrogen and constrained the Au−C/N distances to be equal. This model can be equally well described in $P6/mmm$ with 50/50 occupancy of a single nonmetal site by carbon and nitrogen. In this model, the head to tail ordering of the CN groups is lost. Model C gave the lowest weighted profile R-factor, R_{wp}, and the final fitted profiles are shown in Figures 4 and 5.

Model A yielded inaccurate Au−C and Au−N bond lengths, although they are much closer to the true values

(10) Egami, T. In *Local Structure from Diffraction*; Billinge, S. J. L., Thorpe, M. F., Eds.; Plenum Press: New York, 1998; p 1 and references therein.

Table 2. Structural Parameters[a] and Interatomic Distances for AuCN Determined by Rietveld Analysis, with Au at (0,0,0); and C and N at (0,0,*z*)

model	*T*/K	z_C	z_N	$\langle u_{Au}^2\rangle^{1/2}$/Å	$\langle u_C^2\rangle^{1/2}$/Å	$\langle u_N^2\rangle^{1/2}$/Å	R_{wp}/%	d_{Au-C}/Å	d_{Au-N}/Å	d_{C-N}/Å
A *P*6*mm*	10	0.383(2)	0.610(2)	0.078(3)	0.090(2)	$=\langle u_C^2\rangle^{1/2}$	12.29	1.95(1)	1.98(1)	1.15(2)
A *P*6*mm*	300	0.392(3)	0.618(3)	0.167(3)	0.104(6)	0.187(5)	7.64	1.99(2)	1.94(2)	1.15(2)
B *P*6*mm*	10	0.3868(2)	$=-z_c$	0.077(3)	0.090(2)	$=\langle u_C^2\rangle^{1/2}$	12.30	1.966(1)	$=d_{Au-C}$	1.151(2)
B *P*6*mm*	300	0.3871(2)	$=-z_c$	0.168(2)	0.106(7)	0.183(6)	7.67	1.964(1)	$=d_{Au-C}$	1.145(2)
C *P*6/*mmm*	10	0.3875(2)	$=-z_c$ (Occ=50%)	0.080(3)	0.091(2)	$=\langle u_C^2\rangle^{1/2}$	11.93	1.969(1)	$=d_{Au-C}$	1.144(2)
C *P*6/*mmm*	300	0.3876(2)	$=-z_c$(Occ=50%)	0.167(2)	0.150(1)	$=\langle u_C^2\rangle^{1/2}$	7.52	1.966(1)	$=d_{Au-C}$	1.140(2)

[a] $a = 3.3426(1)$ Å, $c = 5.08238(5)$ Å at 10 K; and $a = 3.3915(1)$ Å, $c = 5.07256(3)$ Å at 300 K.

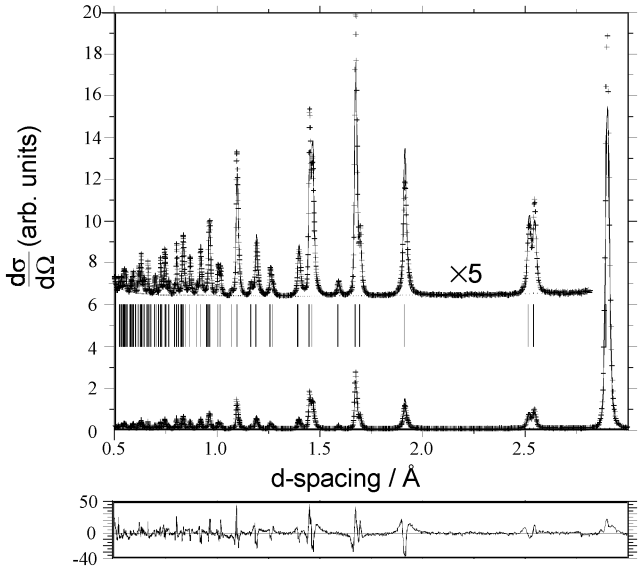

Figure 4. Final fitted profiles (crosses, observed; line, calculated) from Rietveld refinement, model C, for AuCN at 10 K shown in upper frame. Vertical tick lines indicate the positions of the allowed reflections. The lower frame shows the residuals ($I_{obs} - I_{calc}$)/esd) for the fit.

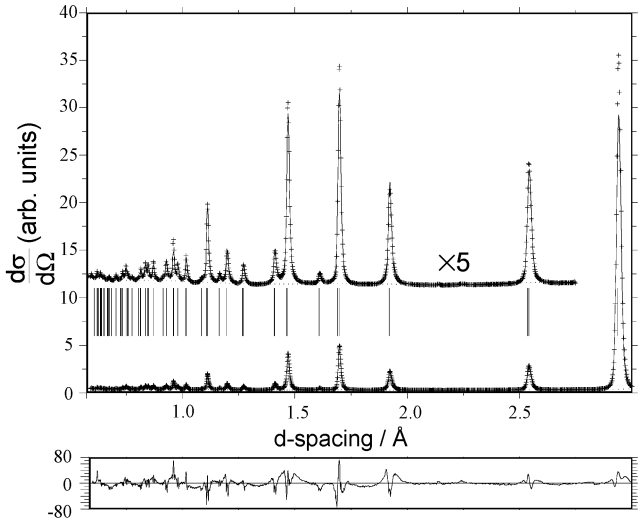

Figure 5. Final fitted profiles (crosses, observed; line, calculated) from Rietveld refinement, model C, for AuCN at 300 K shown in upper frame. Vertical tick lines indicate the positions of the allowed reflections. The lower frame shows the residuals (($I_{obs} - I_{calc}$)/esd) for the fit.

determined by fitting $T(r)$ than those obtained by Bowmaker et al.[1] Models B and C, which constrained the Au−C and Au−N bond lengths to be equal, both gave good Rietveld profile fits and bond lengths close to those determined from $T(r)$. However, both contain the extra information, $d_{Au-N} = d_{Au-C}$, obtained from the $T(r)$ measurement. Model C gives the lowest R_{wp}, consistent with the expected head to tail disorder of CN groups, but this is not definitive, and other techniques are necessary to determine the degree of head to tail disorder. One unusual result from Rietveld refinement is that, although AuCN expands in the *a* direction as the temperature increases from 10 to 300 K, it contracts slightly along *c*. There is thus a negative thermal expansion in one dimension. This behavior reveals the nature of the dominant vibrational motions of the chains. These motions involve long wavelength cooperative motions of relatively large numbers of atoms in a direction perpendicular to the *c* direction. The displacements for these modes are relatively large due to the lack of strong bonding forces between the chains. A rise in temperature causes the population of these modes to increase so that there is an increase in the thermal atomic displacements perpendicular to the chain axis. The Au−C/N and C−N bonds are much stronger so that their length, and hence the overall length of the AuCN chain, changes little with temperature. The transverse atomic displacements are compensated for by pulling the ends of the chain closer together, so that the chain length is preserved, and consequently there is a contraction of the *c* lattice parameter. These sideways motions of the atoms in the chains will increase with temperature, resulting in a higher effective cross section in the *ab* plane for each chain and, hence, expansion of the *a* lattice parameter with temperature. Such motions also explain why $d_{Au-C/N}$ and d_{C-N} found from Rietveld analysis, which yields distances between the mean positions of the atoms, are shorter than $r_{Au-C/N}$ and r_{C-N} found from $T(r)$ which yields a direct measure of interatomic distances.

Close inspection of the fitted profiles in Figures 4 and 5 shows that problems still remain in fitting the Bragg diffraction pattern. One problem, most clearly seen for the 10 K data, is that the four strongest reflections appear to be more intense than those predicted by the model. These are *hk*0 reflections and a possible explanation might be preferred orientation. However, we were able to reject this hypothesis by comparing the profiles from groups of detectors at different azimuthal angles. These showed no significant variation as a function of azimuthal angle. The main source of the apparent discrepancy in intensities is the narrower width of the *hk*0 reflections relative to those of the *hkl* reflections. This gives an insight into one mode of disorder in AuCN, i.e., static displacements (stacking faults) of the chains with respect to each other along their length. This form of disorder is often related to the sample preparation and history, but this is beyond the scope of the paper, because we used a commercially available sample, as did Bowmaker et al.[1] for their diffraction studies. The fact that the *hk*0 reflections are the most intense in the pattern might explain

why the Rietveld refinement of Bowmaker et al.[1] gave a structure with the wrong bond lengths and thermal displacement factors. The basic structure of AuCN is remarkably simple, and only the *z* parameter for the atoms needs to be determined. However, although the *hk*0 reflections dominate the diffraction profile, they contain no information on the value of the *z* parameter for Au, C, and N. The problem is exacerbated in the room temperature data of Bowmaker et al.[1] because many of the *hkl* reflections overlap with the *hk*0 reflections. The accidental degeneracy of these and other reflections at 300 K can be seen by comparing the profiles in Figures 4 and 5. For example, at *d*-spacings of around 1.45, 1.7, and 2.5 Å, it is clear in the 10 K profile that there are pairs of reflections, the *200*/*103*, *110*/*003*, and *101*/*002*, respectively. However, these pairs of reflections become nearly coincident at 300 K. Bowmaker et al.,[1] using a medium resolution constant wavelength diffractometer with much poorer resolution and collecting a much smaller number of Bragg reflections, had effectively very little information in their diffraction pattern for AuCN, and this probably explains why their structure determination is in error.

Structural Modelling

Rietveld analysis confirmed that the average structure could be described in *P*6*mm* or *P*6/*mmm*. This information, together with the lattice parameter *a*, was combined with an effective lattice parameter c ($= r_{C-N} + 2r_{Au-C/N}$), and $z_{C/N}$, obtained from fitting the first two peaks in $T(r)$. Thus, we constructed structural models in space groups *P*6*mm*, with CN head to tail ordering, and in *P*6*mmm*, with no CN ordering. We then calculated $T(r)$ for each model using the program XTAL.[11] The difference in the calculated $T(r)$ is found to be extremely small, and it would be impossible to observe the effect of head−tail disorder in the experimental correlation function, even using our high-quality data. The close similarity of $T(r)$ produced by the two models is due to the equality of the Au−C and Au−N bond lengths. The only differences arise because of the difference between products of scattering lengths, and the maximum difference between $T(r)$ for the fully ordered and fully disordered chains is 2%. We are thus unable to determine whether head to tail disorder occurs in AuCN using total neutron diffraction. Other experiments, possibly NMR or Mössbauer, are necessary to provide a definitive answer on this point.

Figures 6 and 7 show a comparison between $T(r)_{exp}$ and $T(r)_{model}$ for the final models used to describe the structure of AuCN at 10 and 300 K. The parameters for these models are given in Table 3. The agreement between $T(r)_{exp}$ and $T(r)_{calc}$ is excellent at both temperatures and demonstrates that these models give a good description of both the short- and intermediate-range structures in AuCN, as well as the long-range periodic structure. We found that it was necessary to use three different root-mean-square displacements, $\langle u^2\rangle^{1/2}$, to broaden the model correlation function, $T(r)_{model}$, as follows. The first C−N peak in $T(r)_{model}$ was broadened using the width obtained by fitting the first peak in $T(r)_{exp}$. All of the other intrachain peaks were broadened using the width from the fit to the second (Au−C/N) peak in $T(r)_{exp}$. Finally, the interchain peaks were broadened using a larger width which gave optimal agreement between model and experimental correlation functions in the distance range beyond the first two peaks. This third width is larger because there are no chemical bonds between the chains. Table 3 reveals that the $\langle u^2\rangle^{1/2}$ values for the first two types of correlation hardly change with temperature between 10 and 300 K. However, the $\langle u^2\rangle^{1/2}$ value for interchain correlations increases

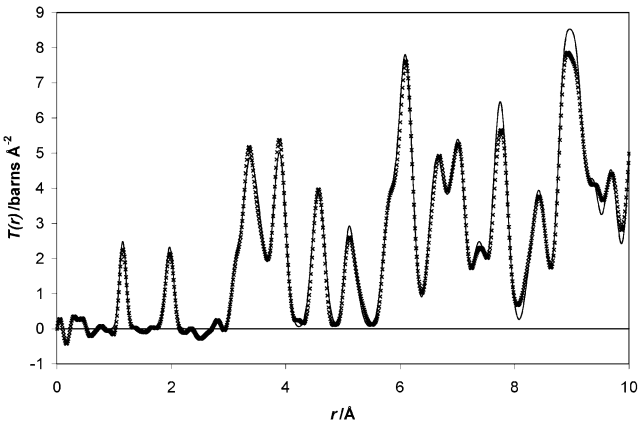

Figure 6. $T(r)_{exp}$ for AuCN (crosses) at 10 K, and $T(r)_{model}$ (continuous line) for our final model incorporating both Rietveld and correlation function information.

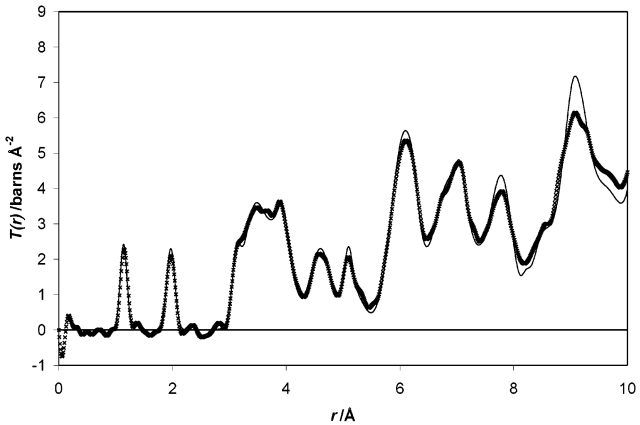

Figure 7. $T(r)_{exp}$ for AuCN (crosses) at 300 K, and $T(r)_{model}$ (continuous line) for our final model incorporating both Rietveld and correlation function information.

Table 3. Structural Parameters[a] Used to Produce the Total Correlation Function, $T(r)_{model}$, for AuCN in *P*6*mmm*

	10 K	300 K
a/Å	3.3426	3.3915
c/Å	5.0981	5.0905
$z_{C/N}$	0.3867	0.3871
$\langle u_{C\equiv N}^2\rangle^{1/2}$/Å	0.022	0.028
intrachain $\langle u^2\rangle^{1/2}$/Å	0.051	0.052
interchain $\langle u^2\rangle^{1/2}$/Å	0.100	0.179
d_{C-N}/Å	1.155	1.150
$d_{Au-C/N}$/Å	1.971	1.970

[a] Au at (0,0,0); C and N at (0,0,*z*) with 50/50 occupancy.

(11) Hannon, A. C. *Rutherford Appleton Laboratory Report*; RAL-93-063; Chilton, Didcot, U.K., 1993.

by a factor of almost two. This again shows that the chains are held together rather weakly.

The $\langle u^2\rangle^{1/2}$ values employed to broaden the different contributions to $T(r)$ for a material, assuming no correlation between atomic motions, are related to the atomic values obtained from Rietveld analysis by

$$\langle u_{ab}{}^2\rangle = \langle u_a{}^2\rangle + \langle u_b{}^2\rangle \quad (2)$$

where $\langle u_{ab}{}^2\rangle$ represents the mean square broadening for the correlation function between a pair of atoms, a and b, and $\langle u_a{}^2\rangle$ is the mean square displacement for atom a. The $\langle u_{C-N}{}^2\rangle^{1/2}$ and $\langle u_{Au-C/N}{}^2\rangle^{1/2}$ values derived from the final Rietveld refinements (Table 1) are much higher than the values found for the first two peaks in $T(r)_{exp}$. This is to be expected, as these peaks correspond to correlations between strongly bonded atoms whose motions are highly correlated. The $\langle u_{ab}{}^2\rangle^{1/2}$ values in Table 1 are, as might be predicted, of the same order as those needed to model the interchain correlations in $T(r)$, but, perhaps less predictably, are slightly larger than the values we used in modeling $T(r)$. The reason for this is that the atomic displacements obtained from Rietveld analysis include the effect of structural order over a length scale longer than that which we have modeled in $T(r)$. At these longer distances, stacking faults, apparent from the *hkl* dependent peak shape, make an additional contribution to disorder.

The structural models we have produced for AuCN at 10 and 300 K account for $T(r)$ over the 0−10 Å length scale extremely well. We have previously been able to achieve such excellent agreement between $T(r)_{exp}$ and $T(r)_{model}$ only when using simple models with few adjustable parameters for ordered crystalline compounds (for example, $Zn_2Mo_3O_8$).[12] The fact that the structural modeling is so much better for AuCN than for AgCN[3] and CuCN[4] shows that in these two materials the static disorder, involving chain displacements, is more complex than that in AuCN.

It is worthwhile considering whether conventional Rietveld analysis could be used in isolation to determine the structure of AuCN, because our final model, model C, does yield good interatomic distances. Total neutron diffraction is both expensive and time-consuming. What are the benefits to the chemist? We believe that the most obvious benefits are the very accurate and direct measurement of bond lengths without recourse to a model, and the experimental proof that the final model used to fit the Bragg diffraction is a good model. It is only possible to be confident of the results from analysis of the Bragg diffraction data from disordered materials when they are checked against the results of total diffraction. In principle, now that we have discovered much more about the nature of the disordered structure of AuCN, further improved analysis of the Bragg diffraction could be envisaged. This would require the writing of computer code for Rietveld analysis, tailored to this specific type of disorder. Among other features, the new software would need to include the correct *hkl* dependent peakshapes. However, a general assault on the structure of a disordered crystalline material without a priori knowledge using only Bragg diffraction, would, we believe, often be more time-consuming than using total diffraction, and would lack the final validation, a direct measurement of interatomic distances, that the latter technique provides.

(12) Hibble, S. J.; Cooper, S. P.; Patat, S.; Hannon, A. C. *Acta Crystallogr.* **1999**, *B55*, 683.

Table 4. M−C/N Bond Lengths in Disordered Group 11 Monocyanides, as Determined by Total Neutron Diffraction.

	CuCN	AgCN	AuCN
$d_{M-C/N}$/Å	1.85	2.06	1.97

There is a question often asked about work on polycrystalline materials, "Couldn't single crystals be grown?" The implication is that single-crystal X-ray diffraction would solve all the structural problems that are unresolved in a powder diffraction study. This is not necessarily the case for disordered materials. Reckeweg and Simon have recently grown single crystals of AgCN.[13] However, the C−N bond length they obtain from single-crystal X-ray diffraction of 1.11(2) Å is too short and has a significant error associated with it.[13] In the case of AgCN, at least, the use of total neutron diffraction has proved to be worthwhile.[3] However, this is an ongoing story, and, as analysis of single-crystal X-ray diffraction from disordered crystalline materials improves, the balance may shift. We await with interest a single-crystal study of the structure of AuCN.

The M−C and M−N bond lengths are equal in CuCN, AgCN, and AuCN, and they follow an interesting sequence, as shown in Table 4. The Au−C distance is in good agreement with that found in compounds containing the $[Au(CN)_2]^-$ complex ion, such as $TlAu(CN)_2$[14] with d_{Au-C} = 1.97 Å, and $RbAu(CN)_2$[15] where three different Au−C distances of 1.91, 1.95, and 1.97 Å are found. The fact that $d_{Ag-C/N}$ is greater than $d_{Au-C/N}$ might at first sight appear surprising. This phenomenon, which can be explained as a consequence of relativistic effects, is seen in other cyanides containing gold and silver. For example, d_{Ag-C} = 2.06 Å in the $[Ag(CN)_2]^-$ complex ion in $TlAg(CN)_2$,[16] and has an average value of 2.10 Å in $RbAg(CN)_2(H_2O)_{0.4}$.[17] In both cases, the Ag−C distances are longer than the Au−C distances in the $[Au(CN)_2]^-$ complex ions found in the closely related gold compounds.[14,15]

Conclusions

We have determined accurate bond distances in the disordered crystalline cyanide, AuCN, by the use of total neutron diffraction, and we have discovered two forms of disorder in AuCN: (1) Short-range disorder between the AuCN chains. This is seen in the total correlation function, $T(r)$, over the 3−10 Å length scale and can be modeled by broadening the interchain correlations to a higher degree than the intrachain correlations. This is evidence for random

(13) Reckeweg, O.; Simon, A. *Z. Naturforsch.* **2002**, *57*, 895.
(14) Blom, N.; Ludi, A.; Buergi, H.-B.; Tichy, K. *Acta Crystallogr.* **1984**, *C40*, 1767.
(15) Schubert, R. J.; Range, K. J. *Z. Naturforsch.* **1990**, *B45*, 629.
(16) Omary, M. A.; Webb, T. R.; Assefa, Z.; Shankle, G. E.; Patterson, H. H. *Inorg. Chem.* **1998**, *37*, 1380.
(17) Kuehnel, S.; Range, K.-J. *Z. Naturforsch.* **1993**, *B48*, 133.

displacements of the chains in the direction of the chain axes. (2) Longer range stacking faults, which result in *hkl* dependent peakshapes.

We suspect a third form of disorder, CN head to tail disorder along the infinite −Au−(CN)−Au−(CN)− chains, but our diffraction results, although consistent with this form of disorder, are unable to provide unequivocal evidence as to its presence.

The temperature dependence of the lattice parameters from Bragg diffraction show a negative thermal expansion in one dimension, along the *c*-axis. The total neutron diffraction results indicate that this is due to long wavelength motions perpendicular to the chain axes.

We have demonstrated once again that total neutron diffraction provides a powerful tool for the study of disordered crystalline materials.[8]

Experimental

Data Collection. Time-of-flight powder neutron diffraction intensities were measured on the GEM diffractometer[9] at the ISIS Facility, Rutherford Appleton Laboratory, Chilton, Didcot, U.K. A powdered sample of 1.3835 g of AuCN (Aldrich) was loaded into a thin-walled, 25-μm, cylindrical vanadium sample holder of nominal 5-mm diameter. The effective density of the sample, as used in the data correction routines, was determined from the sample depth. To obtain the low-temperature data, the sample was cooled to 10 K using a closed-cycle refrigerator. Background runs were collected on the empty can and empty spectrometer and absolute normalization data were collected for a standard vanadium rod.

Data Reduction and Analysis: Rietveld Analysis. Data for Rietveld analysis were obtained by combining the signals from the 90° detector banks and normalizing to the neutron flux, by use of the vanadium rod data. Rietveld refinements were carried out using the program, TF12LS,[18] over the *d*-space range 0.527−3.088 Å with the peak shape modeled by a pseudo-Voigt function convoluted with a double exponential function. The coherent scattering lengths used for Au, C, and N were 0.763×10^{-14} m, 0.6646×10^{-14} m, and 0.936×10^{-14} m, respectively.[19] We used as a starting point for our refinement the structure of AuCN determined by Bowmaker et al.[1] The scale factor and nine polynomial background parameters were refined first, followed by the unit cell, the atomic parameters, displacement factors, and finally the peak shape parameters.

Total Neutron Diffraction. The total neutron diffraction data were obtained by use of three detector banks at nominal scattering angles of 20°, 60°, and 90°. Correction for multiple scattering, attenuation, and inelasticity, and normalization to absolute scattering units was performed using the ATLAS suite of programs.[20,21] The corrected and normalized data from the three detector banks were merged to yield an interference function, $Qi(Q)$, which covered the Q range 0.052−40 Å^{-1}, and this was then extrapolated to $Q = 0$ Å^{-1}.

IC0342043

(18) David, W. I. F.; Ibberson, R. M.; Matthewman, J. C. *Rutherford Appleton Laboratory Report*; RAL-92-032; Chilton, Didcot, U.K., 1992.
(19) Sears, V. F. *Neutron News* **1992**, *3*, 26.
(20) Hannon, A. C.; Howells, W. S.; Soper, A. K. *Inst. Phys. Conf. Ser.* **1989**, *107*, 193.
(21) Hannon, A. C. *ATLAS-online Manual*. http://www.isis.rl.ac.uk/disordered/Manuals/ATLAS/atlas_online.htm.